Photoconductivity in sputter-deposited CdS and CdS-ZnO nanocomposite thin films

Photoconductivity in sputter-deposited CdS and CdS–ZnO nanocomposite thin films

Parinda Vasa[1]**, Praveen Taneja**[1]**, Pushan Ayyub**[1,4]**, B P Singh**[2] **and Rajarshi Banerjee**[3]

[1] Department of Condensed Matter Physics and Material Science, Tata Institute of Fundamental Research, Homi Bhabha Road, Mumbai 400005, India
[2] Physics Department, Indian Institute of Technology, Powai, Mumbai 400076, India
[3] Department of Materials Science and Engineering, The Ohio State University, Columbus, OH 43210, USA

E-mail: pushan@mailhost.tifr.res.in

Abstract

Nanocrystalline CdS and CdS–ZnO thin films were deposited at room temperature using high-pressure radio-frequency magnetron sputtering. The CdS–ZnO nanocomposite film was made up of particles smaller than 2 nm and showed a composite band gap of 2.72 eV. Both samples showed appreciable photoconductivity, extremely fast response and high photostability. We show that the photoresponse in these samples arises mainly from the band-gap transition and excitonic contributions are insignificant. A comparison of the photocurrent response with absorption and photoluminescence data indicates that photocurrent spectroscopy is a simple and extremely useful technique for characterizing systems (such as nanoparticles) with low radiative cross sections.

Currently, there is widespread interest in the optoelectronic properties of nanometre-sized semiconductor particles or quantum dots, which can be used as light emitters, photocells, non-linear optical devices and fast optical switches [1–3]. It is important for such systems to have useful photoluminescence (PL) as well as photoconductivity (PC) characteristics, which can then be tailored through size control. Since the PL yield at room temperature is often rather small in nanoparticle systems [4, 5], we demonstrate the utility of PC spectroscopy (which detects the optical absorption as an electrical signal) for characterizing such systems. Appreciable PC response was obtained in both nanocrystalline (nc) CdS as well as nanocomposite CdS–ZnO thin films, though only the latter showed a strong PL response.

In nanoparticle systems with a characteristic size comparable to the excitonic Bohr radius, one expects high effective quantum efficiencies for PL due to quantum confinement.

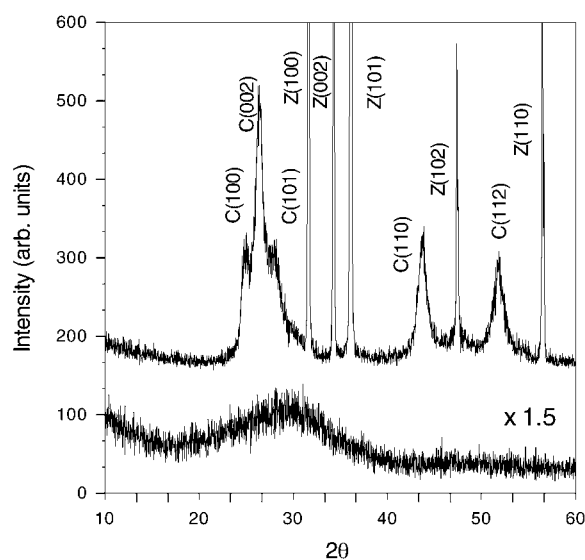[4] Author to whom any correspondence should be addressed.

Figure 1. XRD spectra of the CdS/ZnO sputtering target (top) and a typical sputtered nc thin film deposited on a Si crystal (bottom). Individual reflections of CdS and ZnO are marked by 'C' and 'Z', respectively.

This, however, is usually not realized in the case of bare semiconductor nanoparticles due to the presence of a substantial number of surface electronic states, which provide efficient non-radiative decay channels and lead to a degradation of the optoelectronic properties. A separate report will show that the PL yield from CdS can be enhanced many times by introducing a larger-band-gap material, ZnO, in the form of a nanocomposite. The formation of such a nanocomposite system appears to be a useful alternative to the more commonly adopted process of 'capping' the nanoparticles with a higher-band-gap compound, in order to passivate the surface states.

We showed earlier that rf/dc magnetron sputtering at relatively low substrate temperatures and high sputter-gas pressures leads to uniform, nearly stoichiometric, nc thin films of metals, oxides, sulphides, nitrides etc [6–8]. Pure CdS and CdS–ZnO were rf-sputtered onto Si(100) or quartz substrates maintained at 300 K at Ar pressures of $\sim 10^{-1}$ mbar. The sputtering target was a 50 mm compacted pellet of CdS (99.99%) or a mixture of CdS and ZnO (2:3 mole ratio). The x-ray diffraction (XRD) spectrum of the CdS–ZnO thin film, recorded using a Siemens D500 powder diffractometer with a Cu Kα target, shows a very broad feature and no identifiable reflections of either CdS or ZnO (figure 1, bottom). In the same figure, the XRD spectrum of the CdS/ZnO sputtering target is also shown for comparison. The XRD data suggest that the resulting material is probably a nanocomposite of CdS and ZnO with the average particle size for both phases being less than ≈ 2 nm. This conclusion is confirmed by transmission electron micrographs (figure 2) that show a uniform distribution of closely aggregated nanoparticles with an average size of 1–2 nm. A detailed analysis of the selected-area electron diffraction patterns (not shown here) confirms the presence of CdS and ZnO as *distinct* crystallographic phases. The presence of Cd, Zn, S and O (in nearly stoichiometric proportion) in the nc thin films is confirmed by elemental analysis (EDS) using the TEM. The XRD of the pure CdS thin film shows only the (002) reflection of hexagonal CdS in addition to a broad hump, indicating a preferential (002) orientation for the CdS nanoparticles [9].
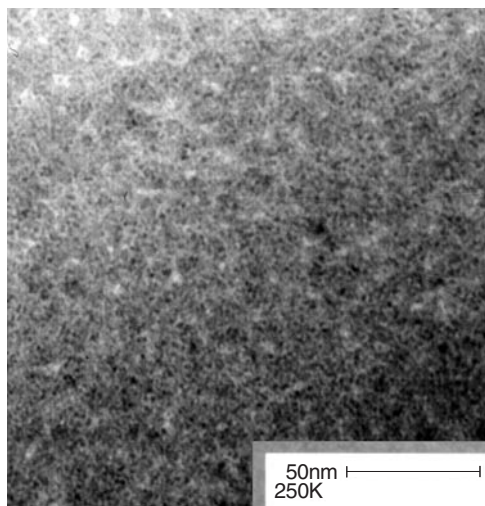
Figure 2. A transmission electron micrograph ($\times 250\,000$) of a typical CdS–ZnO nanocomposite thin film deposited on Si.

Figure 3 shows the optical absorption spectra of CdS and CdS–ZnO nanocomposite thin films deposited on quartz, recorded in the 200–800 nm wavelength range using a Shimadzu UV-2100 spectrophotometer. The long-wavelength oscillations are due to interference of light undergoing reflections at the front and back surfaces of the films. The interference pattern was used to calculate the film thickness (t). We obtain: $t = 0.384$ μm for the CdS film and $t = 0.794$ μm for the CdS–ZnO film. (In the latter case, a weighted average of the refractive indices of CdS and ZnO was used for the thickness calculation.) The band gap (E_g) was calculated from the optical absorption edge using the equation for direct-gap semiconductors [10]. For the CdS film, $E_g = 2.42$ eV, which is close to the bulk value (2.5 eV), in agreement with the XRD data. For the CdS–ZnO nanocomposite, $E_g = 2.72$ eV, which is much lower than the gap in bulk ZnO (3.35 eV at 300 K). Note that the band gap for ZnO should usually get further blue-shifted due to size reduction. Therefore, the observed E_g is either due to CdS nanoparticles or corresponds to the CdS–ZnO composite material. If we ascribe it to nano-CdS, the observed blue-shift should correspond to a CdS particle diameter of ≈ 5 nm. Since both XRD and transmission electron microscopy indicate a much smaller particle size, we may conclude that the band gap of 2.72 eV corresponds to a composite system of CdS and ZnO nanoparticles [1, 4, 11] with an average crystallite size less than 2 nm.

The PL emission is quite weak in pure CdS nanoparticles due to non-radiative surface states [4]. On passivating the CdS nanoparticles by *in situ* hydrogenation we observed a broad-band multi-peak PL emission (at 300 K) in the 480–600 nm range, the spectrum being obtained at the peak excitation wavelength of 450 nm [9]. The highest-energy peak at 514 nm corresponds to the band gap, while the lower-energy peaks originate from excitonic transitions or defect states. At 300 K, the PL from the CdS–ZnO nanocomposite was much stronger than in pure CdS, possibly due the passivating effect of ZnO. The PL excitation spectrum for this sample is shown in figure 4. The maximum PL yield in this sample occurred at an excitation frequency of 355 nm, the corresponding emission showing a broad-band structure in the 400–600 nm range.

PC measurements were carried out using the emission from a 150 W Xe arc lamp that was chopped at 121 Hz and monochromatized. A beam splitter directed a part of the incident light to a PMT, whose output was fed to a lock-in amplifier. The dark resistance of both samples (CdS and CdS–ZnO), measured across sputtered silver electrodes separated by 1 mm, was found to be greater than 20 MΩ. A dc bias voltage was applied to the electrodes, in series with
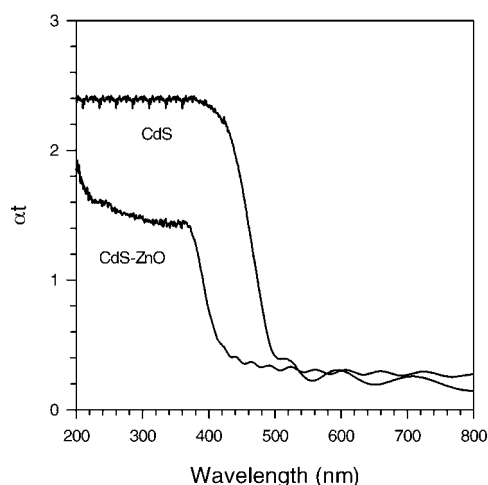
Figure 3. Optical absorption spectra of CdS and CdS–ZnO nanocomposite films deposited on quartz.
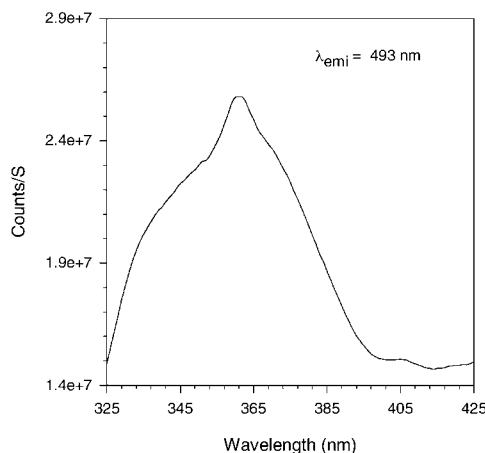
Figure 4. The PL excitation spectrum for a typical CdS–ZnO sample deposited on Si. The emission wavelength was kept fixed at 493 nm.
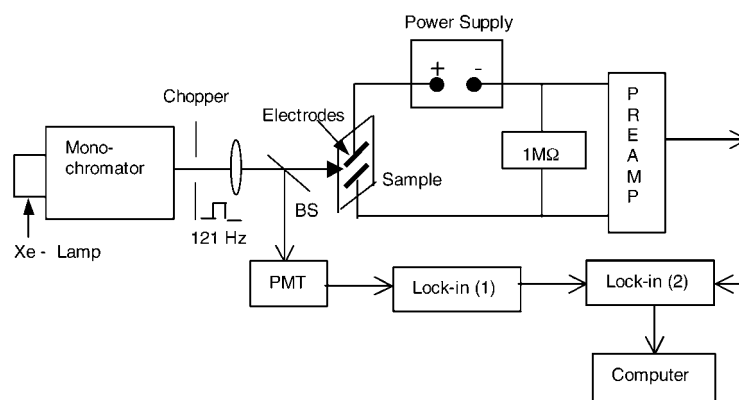

Figure 5. A schematic diagram of the experimental set-up used for the measurement of the PC in nc thin films as a function of incident wavelength (BS = beam splitter).

a 1 MΩ resistance. The change in the potential drop across the 1 MΩ resistance was detected, as a function of the incident wavelength, by a preamplifier that fed a second lock-in amplifier. Signals from both of the lock-ins were fed to a computer. The photocurrent was normalized with respect to the lamp emission at all wavelengths. A schematic diagram of the experimental set-up is shown in figure 5.

Incident light of appropriate energy produces charge carriers, which may actually get trapped by the defect states before they can migrate to the electrodes. Such traps reduce the average drift velocity and the photocurrent, and may lead to a significant decrease in the quantum efficiency [12]. This effect can be countered by applying a bias voltage across the electrodes. Both the drift velocity and photocurrent increase linearly with the bias voltage until saturation occurs, provided that no charge injection takes place from the electrodes to maintain charge neutrality within the sample. However, at high voltages some carriers are injected from the electrodes, which might prevent photocurrent saturation and result in a much larger gain.
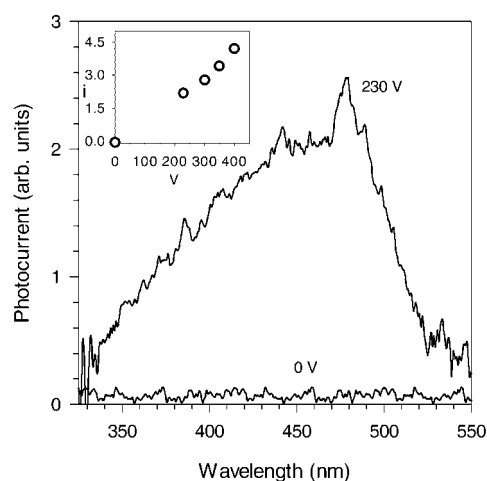
Figure 6. The photocurrent spectrum in nc CdS thin film (on a quartz substrate) for two different bias voltages. The inset shows the variation in photocurrent at 436 nm with the bias voltage.
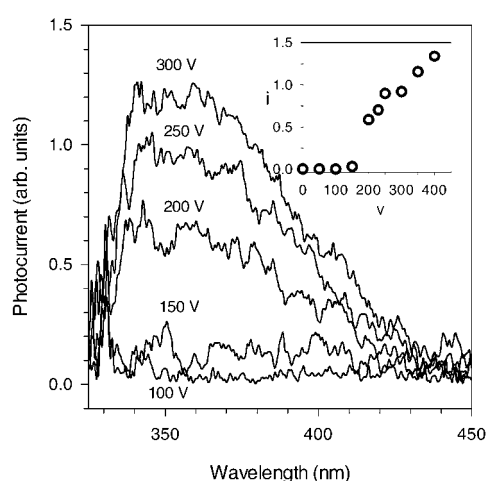
Figure 7. The photocurrent spectrum in CdS–ZnO nanocomposite thin film (on a quartz substrate) for different bias voltages. The inset shows the variation in photocurrent at 366 nm with the bias voltage.

The photoresponse spectra of CdS and CdS–ZnO nanocomposite thin films for different bias voltages are shown in figures 6 and 7, respectively. The PC is low but measurable when the bias voltage is less than 100 V (which corresponds to 1 kV cm^{-1}). At 1.5 kV cm^{-1}, a broadband photoresponse was observed in the wavelength range of 325–530 nm (3.83–2.34 eV) in CdS and in the 325–440 nm (3.83–2.83 eV) range in CdS–ZnO. The somewhat noisy response can be attributed to the trapping of the charge carriers and space-charge build-up. The photocurrent increases with increasing voltage but the wavelength dependence remains qualitatively similar. No electroluminescence was observed in these samples over the entire range of operating voltage. Any contribution from the substrate may be ruled out since the bare quartz substrate exhibited no photoresponse at even higher applied voltage.

A comparison of the optical absorption, PL and PC data indicates that the long-wavelength edge of the photocurrent matches the optical absorption edge for both samples. Note, however, that the sharp drop in the photocurrent in nc CdS–ZnO below ∼330 nm (figure 7) occurs due to the short-wavelength edge of the Xe lamp spectrum. In the case of nc CdS, on the other hand, the more gradual drop in the photocurrent that occurs below ∼450 nm can be ascribed to a reduction in the density of states in the conduction band at corresponding energies.

The insets in figures 6 and 7 show that at a fixed wavelength, the photocurrent increases linearly with voltage above a certain threshold. The maximum photocurrent measured was 14 pA in CdS (at ∼450 nm) and 12.9 pA in CdS–ZnO (at ∼355 nm), which corresponds to an ≈4% change in the actual sample resistance. The peak wavelengths for PC match the peak excitation wavelengths in the respective PL spectra. Therefore the ground states involved in PL are same as those that give rise to PC. No saturation of photocurrent was observed, but a breakdown occurred in the CdS–ZnO sample at 450 V. A time response study showed that the photocurrent followed the change in the light intensity instantaneously (in less than 50 μs). No photocurrent bleaching was observed over 5 min, but a slow increase in the PC with time may be attributed to ohmic heating of the sample by the incident light. The sputter-deposited CdS and CdS–ZnO films are therefore photostable, at least on the timescale of minutes. Also, the photocurrent was found to vary linearly with light intensity.

The long-wavelength edge of the photocurrent (530 nm in CdS, 440 nm in CdS–ZnO) corresponds closely to the optical absorption edge (515 nm in CdS, 457 nm in CdS–ZnO). This indicates that the photoresponse in these samples is related to the band-gap transition. Being electrically neutral, excitons do not normally contribute to the photocurrent [13] but they may dissociate at higher applied fields and show a photoresponse at wavelengths larger than the band edge. Since we do not observe a change in the photoresponse spectrum with bias voltage, we may rule out excitonic contributions to the PC. This conclusion is based on the calculation of the size dependence of the energy spectrum of bound excitons due to Schmidt and Weller [14]. In 2 nm CdS particles, the ground-state energy of the excitons, measured from the bottom of the conduction band in the bulk material, is about 400 meV. We, therefore, do not expect any significant excitonic dissociation at room temperature.

In conclusion, we have observed appreciable PC in sputter-deposited CdS and CdS–ZnO nanocomposite thin films. The CdS film is made up of comparatively larger particles with a preferred (002) orientation. The CdS–ZnO thin film consists of particles smaller than 2 nm and shows a composite band gap of 2.72 eV. As there is a close correspondence between the PC data and the spectral features (peak response, band edge) obtained from optical absorption and PL, it is clear that photocurrent spectroscopy provides an alternative technique for the characterization of semiconductors. Since the generation of photocarriers does not depend on radiative recombination, it is particularly useful for materials with lower cross section for radiative relaxation.

References

[1] Pavesi L, Negro L D, Mazzoleni C, Franzo G and Priolo F 2000 *Nature* **408** 440
[2] Ng W L, Lourenco M A, Gwilliam R M, Ledain S, Shao G and Homewood K P 2001 *Nature* **410** 192
[3] Artemyev M V, Sperling V and Woggon U 1997 *J. Appl. Phys.* **81** 6975
[4] Woggon U 1997 *Optical Properties of Semiconductor Quantum Dots (Springer Tracts in Modern Physics vol 136)* (Berlin: Springer) chs 3, 9
[5] Erley G, Gorer S and Penner R M 1998 *Appl. Phys. Lett.* **72** 2301
[6] Chandra R, Taneja P and Ayyub P 1999 *Nanostruct. Mater.* **11** 505
[7] Chandra R, Taneja P, Ayyub P, Dey G K and Kulshreshtha S K 1999 *Nanostruct. Mater.* **11** 1171
[8] Ayyub P, Chandra R, Taneja P, Sharma A K and Pinto R 2001 *Appl. Phys.* A **73** 67
[9] Taneja P, Vasa P and Ayyub P 2001 *Mater. Lett.* at press
[10] Singh J 1995 *Semiconductor Optoelectronics—Physics and Technology* (New York: McGraw-Hill) p 191
[11] Meng X Q, Zhen W, Guo J P and Fan X J 2000 *Appl. Phys.* A **70** 421
[12] Bube R 1960 *Photoconductivity of Solids* (New York: Wiley) chs 1, 3, 8
[13] Tomm J W, Ullrich B, Qiu X G, Segawa Y, Ohtomo A, Kawasaki M and Koinuma H 2000 *J. Appl. Phys.* **87** 1844
[14] Schmidt H M and Weller H 1986 *Chem. Phys. Lett.* **129** 615